한국소음진동공학회 2001년도 춘계학술대회논문집, pp. 72~77.

자기유변유체댐퍼를 이용한 대형 구조물의 풍하중에 대한 반능동 제어

Semi-Active Control of Wind-Induced Vibration of Tall Building Using Magneto-Rheological Dampers

윤정방* 구자인** 김상범*** 전준보****

Chung-Bang Yun* Ja-In Gu** Saang Bum Kim*** Jun-Bo Jeon****

국문요약

고층 빌딩의 풍하중에 의한 진동을 제어하기 위하여 MR 유체감쇠기를 이용한 반능동 제어 시스템의 설계에 대하여 연구하였다. 제안된 설계기법의 효율성을 검증하기 위하여 ASCE benchmark 구조물을 대상으로 수치 모의해석을 수행하였다. 유전자 알고리즘을 사용하여 MR 감쇠기의 76층 빌딩 내에서의 최적위치와 용량을 결정하였으며, clipped optimal control 제어기법을 사용하여 가속도 되먹임 구조를 갖는 MR 감쇠기의 제어 알고리즘을 구성하였다. 수치 모의 해석 결과로부터 MR 감쇠기는 ATMD와 유사한 제어 성능을 가지고 있으며 매우 작은 규모의 파워 시스템만으로 운영이 가능한 효율적이고 안정적인 제어 시스템임을 확인할 수 있었다.

1. Introduction

Slender and tall buildings are very sensitive to wind loads. To enhance the human comfort under wind loads, tuned mass dampers and active tuned mass dampers have been widely used for response control of wind excited tall buildings(Yang & Samali 1983, Koh et al. 1998, Kim & Yun 2000).

In this study, a recently developed semi-active control system using MR dampers is applied to control the wind-induced vibration of tall buildings. A numerical simulation study is carried out on a 76-story buildings, which was proposed for benchmark studies on control of wind-induced vibration by ASCE. Genetic algorithm is used to determine the optimal locations and capacities of the MR dampers. The performance of the semi-actively controlled case is compared with those of the passively and actively controlled cases, and the effectiveness of the semi-actively controlled MR dampers is discussed.

2. Model of Control System

2.1 Modeling of Structure

Referring to the 76-story building structure for the ASCE benchmark problem of wind vibration control as in Figure 1, the dynamic behavior of the structure with a set of MR dampers can be modeled as

$$\mathbf{M}\ddot{\mathbf{y}}(t) + \mathbf{C}\dot{\mathbf{y}}(t) + \mathbf{K}\mathbf{y}(t) = \mathbf{f}(t) + \mathbf{B}\mathbf{f}_{MR}(t, v_{app}) \qquad (1)$$

where $\mathbf{y}(t)$, $\mathbf{f}(t)$, $\mathbf{f}_{MR}(t, v_{in})$, and v_{app} = vectors for displacement, wind force, force from MR dampers, and applied voltage; $\mathbf{M}$, $\mathbf{C}$, and $\mathbf{K}$ = mass, damping, and stiffness matrices; and $\mathbf{B}$ = Boolean matrix representing the effects of the MR dampers.

The problem organizer constructed a reduced system with 23 DOF's using the state order reduction method for computational efficiency. The selected DOF's are the horizontal displacements of 23 floors: i.e. 3, 6, 10, 13, 16,

* 한국과학기술원 교수
** 삼성정보기술연구소 연구원
*** 한국과학기술원 연구원
**** 한국과학기술원 석사과정

20, 23, 26, 30, 33, 36, 40, 43, 46, 50, 53, 56, 60, 63, 66, 70, 73 and 76th floors. The corresponding state and measurement equations are

$$\dot{\mathbf{x}}(t) = \mathbf{A}\mathbf{x}(t) + \mathbf{B}_d\mathbf{f}_{MR}(t, v_{in}) + \mathbf{B}_f\mathbf{f}(t) \quad (2)$$
$$\mathbf{y}_c(t) = \mathbf{C}_c\mathbf{x}(t) + \mathbf{D}_{cd}\mathbf{f}_{MR}(t, v_{in}) + \mathbf{D}_{cf}\mathbf{f}(t)$$
$$\mathbf{y}_m(t) = \mathbf{C}_m\mathbf{x}(t) + \mathbf{D}_{md}\mathbf{f}_{MR}(t, v_{in}) + \mathbf{D}_{mf}\mathbf{f}(t) + \mathbf{v}(t)$$

where $\mathbf{x}(t)$, $\mathbf{y}_c(t)$, $\mathbf{y}_m(t)$, and $\mathbf{v}(t)$ = state, control signal, measured signal, and measurement noise vectors; and $\mathbf{A}$, $\mathbf{B}_d$, $\mathbf{B}_f$, $\mathbf{C}_c$, $\mathbf{D}_{cd}$, $\mathbf{D}_{cf}$, $\mathbf{C}_m$, $\mathbf{D}_{mu}$, and $\mathbf{D}_{mf}$ = system matrices.

2.2 Model of MR Fluid Damper

The MR has several unique characteristics, such as high dynamic yield strength, wide operating temperature range, requirement of small voltage to control the damper force, and short response time(Carlson et al. 1994). Many researchers studied on modeling of the MR fluid. In this paper, the bi-viscous model shown in Figure 2(Stanway et al. 1996) is used to predict the behavior of the MR damper. Then the damper force can be modeled as

$$f_{MR} = \begin{cases} c_1\dot{y}_{MR}, & if \ \ |\dot{y}_{MR}| < \dot{y}_{MRy} \\ c_0\dot{y}_{MR} + f_{MRy}\,\mathrm{sgn}(\dot{y}_{MR}), & if \ \ |\dot{y}_{MR}| > \dot{y}_{MRy} \end{cases} \quad (3)$$

where $\dot{y}_{MR}$ is velocity of the MR damper, $\dot{y}_{MRy}$ is yield velocity, f_{MRy} is yield force; c_0 and c_1 are damping coefficients for post- and pre-yield conditions.

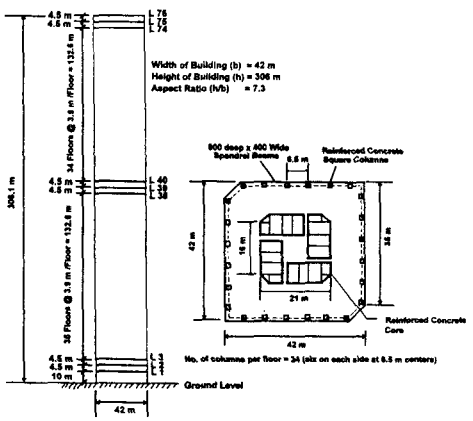

Figure 1 Benchmark structure of wind vibration control

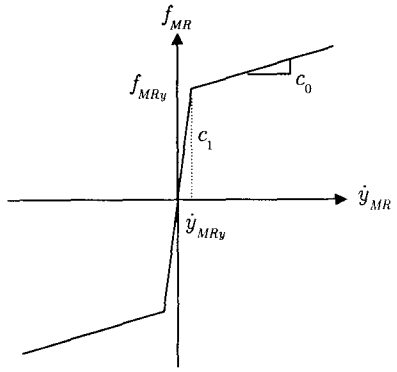

Figure 2 Bi-viscous model of MR damper

The functional dependence of the parameters on the input voltage v_{in} to the damper is considered as follows (Dyke et al. 1998)

$$f_{MRy}(v_{in}) = f_{MRya} + f_{MRyb}v_{in}$$
$$c_1(v_{in}) = c_{1a} + c_{1b}v_{in} \quad (4)$$

The dynamics involved in the system reaching equilibrium due to the resistance and inductance in the circuit are considered through the first order filter suggested by Spencer et al. (1997)

$$\dot{v}_{in} = -\eta(v_{in} - v_{app}) \quad (5)$$

where v_{app} is the applied voltage

The MR dampers with a capacity of 200kN and a dynamic ratio of 10 for each unit, which were designed by Lord Corporation and tested at University of Notre Dame (Spencer et al. 1997), are selected for this study. Damper parameters are shown in Table 1.

2.3 Model Reduction and State Observer

Before designing the controller, two stages of pre-design were carried out. The first stage is for another model reduction from 23 DOFs to 5 DOFs for the computational efficiency in the control process. The DOFs of the reduced system are the horizontal displacements of 16, 30, 40, 60 and 76th floors. The second is for design of observer. The Kalman-Bucy filter is used to estimate the state from the measured signal as (Goodwin & Sin 1984)

Table 1 Parameters of bi-viscous model

Parameter	Value	Parameter	Value
c_{1a}	10000 kNs/m	f_{MRya}	20 kN
c_{1b}	18000 kNs/mV	f_{MRyb}	36 kN/V
$\dot{y}_{MRy}$	0.002 m/s	c_0	50 kNs/m
η	50 sec^{-1}		

$$\dot{\hat{\mathbf{x}}}_r = \mathbf{A}_r\hat{\mathbf{x}}_r(t) + \mathbf{B}_{rd}\mathbf{f}_{MR}(t) + \mathbf{L}_{obs}(\mathbf{y}_m(t) - \mathbf{C}_{mr}\hat{\mathbf{x}}(t) - \mathbf{D}_{mrd}\mathbf{f}_{MR}(t)) \quad (6)$$

where $\hat{\mathbf{x}}_r$ = estimated state vector; $\boldsymbol{y}_m$ = measured signal $[\ddot{y}_{50}, \ddot{y}_{70}, \ddot{y}_{76}]^T$; $\mathbf{L}_{obs} = (\mathbf{P}_{obs}\mathbf{C}_{mr}^T + \mathbf{S}_{obs})\mathbf{R}_{obs}^{-1}$ = observer gain matrix, which can be obtained by solving the following algebraic Riccati equation for $\mathbf{P}_{obs}$

$$\bar{\mathbf{A}}_r\mathbf{P}_{obs} + \mathbf{P}_{obs}\bar{\mathbf{A}}_r^T - \mathbf{P}_{obs}\mathbf{C}_{mr}^T\mathbf{R}_{obs}^{-1}\mathbf{C}_{mr}\mathbf{P}_{obs} + \mathbf{Q}_{obs} - \mathbf{S}_{obs}\mathbf{R}_{obs}^{-1}\mathbf{S}_{obs}^T = \mathbf{0} \quad (7)$$

where

$$\bar{\mathbf{A}}_r = \mathbf{A}_r - \mathbf{C}_{mr}^T\mathbf{R}_{obs}^{-1}\mathbf{S}_{obs}^T$$

$$\begin{bmatrix}\mathbf{Q}_{obs} & \mathbf{S}_{obs}\\ \mathbf{S}_{obs}^T & \mathbf{R}_{obs}\end{bmatrix}\delta(\tau) = E\left[\begin{Bmatrix}\mathbf{B}_{rf}\mathbf{f}_s(t)\\ \mathbf{D}_{rf}\mathbf{f}_s(t) + \mathbf{v}_r(t)\end{Bmatrix}\begin{Bmatrix}\mathbf{B}_{rf}\mathbf{f}_s(t)\\ \mathbf{D}_{rf}\mathbf{f}_s(t) + \mathbf{v}_r(t)\end{Bmatrix}^T\right]$$

3. Design of Controller

3.1 Clipped Optimal Control for MR Dampers

Conventional control algorithms based on the ordinary linear optimal control have inherent limitations for applying to the semi-active control. Hence, the clipped optimal control proposed for semi-active control system by Sack & Patten (1994) and Dyke et al. (1998) is employed in this study. To calculate the desired optimal control force f_{LQG} , a linear optimal controller is designed using the linear quadratic Gaussian(LQG) control theory based on the measured structural acceleration $\ddot{y}$ and the measured damper force f_{MR} as

$$\boldsymbol{f}_{LQG} = L^{-1}\left\{-\mathbf{K}_{LQG}(s)L\begin{Bmatrix}\ddot{\boldsymbol{y}}\\ f_{MR}\end{Bmatrix}\right\} \quad (8)$$

where $L\{\cdot\}$ is the Laplace transform, $\mathbf{K}_{LQG}(s)$ is the transfer function of the ordinary LQG controller. The control variables are taken as $\boldsymbol{y}_c = [\ddot{y}_3, \ddot{y}_{30}, \ddot{y}_{50}, \ddot{y}_{56}, \ddot{y}_{60}, \ddot{y}_{66}, \ddot{y}_{70}, \ddot{y}_{73}, \ddot{y}_{76}]^T$.

The force generated by the MR damper cannot be directly controlled to get the desired optimal control force f_{LQG} , only the command voltage to the MR damper v_{app} can be directly controlled to increase or decrease the force produced by the device. Hence, to induce the MR damper to generate approximately the desired optimal control force, the voltage is selected as follows. If the device generates the desired optimal control force(*i.e.*, $f_{MR} = f_{LQG}$), the command voltage remains at the present level. However, if f_{MR} is smaller than f_{LQG} and their signs are same, v_{app} increases to the maximum level to make f_{MR} increase. Otherwise, the command voltage is set to zero. This algorithm can be expressed using Heaviside step function as (Dyke et al. 1998).

$$v_{app} = v_{\max}H\{(f_{LQG} - f_{MR})f_{MR}\} \quad (9)$$

3.2 Design of Locations and Capacities of MR Dampers by Genetic Algorithm

The performance of the MR dampers depends strongly on their locations in the structure. The determination of the locations and capacities (numbers of units) of the MR dampers is an integer programming, which requires extensive search and heavy computational efforts. Moreover, the total number of the possible locations is so great for the 76-story building and the cost surfaces may be extremely complex. The genetic algorithm has some advantages that match well with the present problem such as, (1) it optimizes with continuous or discrete parameters; (2) it does not require derivative information; (3) it deals with a large number of parameters; (4) it optimizes parameters with extremely complex cost surfaces; and (5) it can jump out of a local optimum (Goldberg 1989). For these reasons, the generic algorithm was used to find the optimal locations and capacities of MR dampers in this study. To reduce the computational time, a preliminary study was carried out on 3 cases, such that (1) MR dampers placed on the lower floors (3, 6, 10, 13, and 16th floors), (2) MR dampers placed on the middle (33, 36, 40, 43, and 46-th floors), and (3) MR dampers placed on the higher floors (63, 66, 70, 73, and 76th floors). The results show that it

is more effective to place the MR dampers at the higher floors. Therefore, only 63, 66, 70, 73, and 76th floors were considered in determining the capacities of the MR dampers using genetic algorithm. The objective function was defined considering the performance criteria related to acceleration, because the purpose of vibration control under wind loads is mainly to reduce the discomfort of the occupants. Finally, the optimum number of the MR dampers on each floor is determined as 2, 7, 5, 4, and 3 on 63, 66, 70, 73, and 76th floors, respectively.

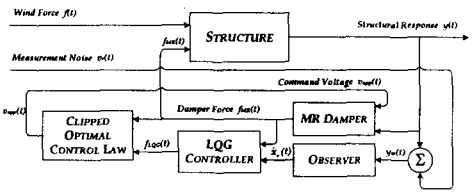

Figure 3 Schematic diagram of the clipped optimal controller

4. Numerical Simulation Study

A numerical simulation study is carried out on the benchmark structure subjected to wind loads proposed by Yang, et al. (2000). It is a 76-story concrete office tower, and it is modeled as a system with 23 DOF's for structural analysis by the problem organizer. Detailed data related to this problem are given at the web site of the problem organizer. In this study, it is further reduced to a system with 5 DOF's (i.e. 10 dimensional state vector) using the state order reduction method for the computational efficiency in the control process.

Wind force data in along- and across-wind directions were determined from wind tunnel tests, which were performed by Samali et al. (1999). For this benchmark problem, 900 seconds of across-wind data are given for the computation of the structural response. In these wind data, the mean wind force on each floor has been removed, since it produces only the static deflection of the building. The reference mean wind speed, V_r, at the height of 10 meters above the ground is assumed to be 13.5 m/s, which represents the serviceability level related to the comfort of the occupants. Ten performance indices among twelve defined by the problem organizer are used in this study. They are J1 and J2 for rms acceleration performance, J3 and J4 for rms displacement performance, J7 and J8 for peak acceleration performance, and J9 and J10 for peak displacement performance. The smaller the indices, the better the control performance.

Figure 4 shows time histories of structural responses with and without semi-active control, and Figure 5 shows time histories of the forces of the MR dampers. The peak and RMS responses of the 76-story building with passive MR dampers and semi-actively controlled MR dampers are shown in Tables 2 and 3. For simplicity only the responses of 30, 60, 75 and 76th floors are presented. Similar results for the cases with a tuned mass damper (TMD) and an active tuned mass damper (ATMD) obtained by Yang et al. (2000) are also shown for comparison. The performance indices for various control methods are compared in Table 4. The maximum damper forces are shown in Table 5. It is found that the semi-active control system employing MR dampers reduces the peak and RMS displacements of the building by 28-33% and 45-47% of the uncontrolled cases, and the peak and RMS acceleration by 49-58% and 61-65%. The improvement for the acceleration reduction is more significant, because the controllers are designed mainly for the reduction of the acceleration. The maximum allowable floor acceleration is 15cm/sec^2 (or 5cm/sec^2 in RMS value), based on the design code for office buildings. It is observed that the semi-actively controlled MR dampers satisfy the design requirement. The performances of the semi-active control system with MR damper are found to be much better than those with a TMD, while they are fairly comparable to those with and ATMD. The performance indices of the MR dampers related to the peak accelerations (J7 and J8) are slightly higher than those with and ATMD, while the one related to the RMS acceleration (J2) is slightly lower.

The performance of the MR dampers may vary significantly with the exciting force level, since they are nonlinear devices. Thus, additional analyses are carried out on the cases with same control devices but for different wind loads: i.e. $0.5F_{WD}$, $1.5F_{WD}$ and $2.0F_{WD}$,where F_{WD} is the wind force for the case with V_r being 13.5 m/s. The performance indices shown in Table 6 indicate that the semi-active control system with MR dampers is fairly robust to the variations of the exciting force level.

5. Concluding Remarks

MR dampers are studied as semi-active control devices for a tall building subjected to wind loads. Clipped optimal control is used to control the strength of the magnetic filed applied to the dampers. Genetic algorithm is used for the optimal design of the controller locations and capacities. To verify the applicability of the MR dampers and the suggested control algorithm, a numerical simulation study is carried out on the ASCE benchmark problem on wind-excited building. The results indicate that the present semi-active control system employing magneto-rheological (MR) fluid dampers can reduce the wind-induced vibration very effectively. The control performances of the MR dampers for wind is found to be fairly comparable to those of the system with an ATMD.

ACKNOWLEDGEMENT: The authors gratefully acknowledge the financial support to this research from the BK21 Project entitled "Advanced Structural Engineering Technology Research" sponsored by the Korea Research Foundation.

REFERENCES

Carlson, J.D. & Weiss, K.D. 1994. A growing attraction to magnetic fluids. *Machine Design*: 61-64.

Dyke, S.J. Spencer, B.F. Jr. Sain, M.K. & Carlson, J.D. 1998. An experimental study of MR dampers for seismic protection. *Smart Material and Structures* 7: 693-703.

Symans, M.D. & Constantinou, M.C. 1999. Semi-active control systems for seismic protection of structures: a state-of-the-art review. *Engineering Structures* 21: 469-487.

Goodwin, G.C. & Sin K.S. 1984. *Adaptive Filtering, Prediction, and Control.* Englewood Cliffs, New Jersey: Prentice-Hall.

Kim, S.B. & Yun, C.B. 2000. *Sliding mode fuzzy control with disturbance estimator for wind-induced vibration control; Proc. of 2nd European Conference on Structural Control, Champ-Sur-Marne, France, 3-6 July 2000.*

Koh, H.M. Park, S. Park, W. Park, K.S. & Km, Y.S. 1998. *Active vibration control of air traffic control tower at Inchon international airport under wind excitation; Proc. of the 2nd World Conference on Structural Control, Kyoto, Japan.*

The Math Works, Inc. 1994. *MATLAB.* Natick, Massachusetts: The Math Works, Inc.

Spencer, B.F. Jr Dyke, S.J. Sain, M.K. & Carlson, J.D. 1997. Phenomenological model for magneto-rheological dampers. *Journal of Engineering Mechanics*: 230-238.

Spencer, B.F. Jr Yang, G. Carlson, J.D. & Sain, M.K. 1998. *Smart dampers for seismic protection of structures: a full-scale study; Proc. of the 2nd World Conference on Structural Control, Kyoto, Japan.*

Stanway, R. Sproston, J.K. & El-Wahed, A.K. 1996. Application of electro-rheological fluids in vibration control: a survey. *Smart Material and Structures* 5(4): 464-482.

Wereley, N.M. Pang, L. & Kamath., G.M. 1998. Idealized hysterisis modeling of electro-rheological and magneto-rheological dampers. *Journal of Intelligent Material Systems and Structures* 9: 642-649.

Yang, J.N. & Samali, B. 1983. Control of tall buildings in along-wind motion. *Journal of Engineering Mechanics, ASCE* 121(12): 1330-1339.

Yang, J.N. Agrawal, A.K. Samali, B. & Wu, J.C. 2000, A benchmark problem for response control of wind-excited tall buildings. *Benchmark Problem Package Available at the World Wide Website: http:// gram.eng.uci.edu/ civil/faculty/yang/index.html*

Goldberg, D.E. 1989. Genetic Algorithms in Search, Optimization, and Machine Learning. Addison-Wiley.

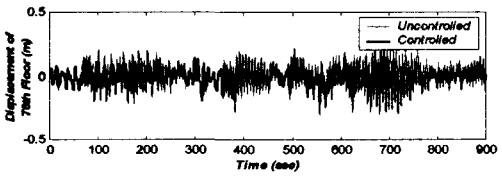

(a) Displacements of 76th floor

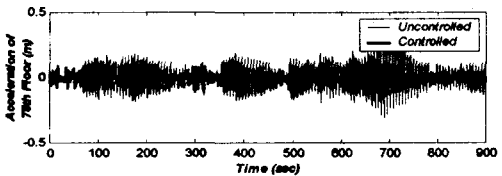

(b) Accelerations of 75th floor

Figure 4 Time histories of the structural responses with and without semi-active control

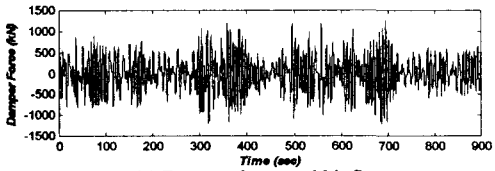

(a) Damper force at 66th floor

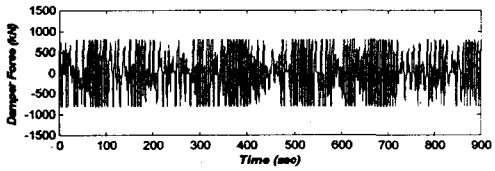

(b) Damper force at 73rd floor

Figure 5 Time histories of MR damper forces

Table 2 Peak response quantities of 76-story building with various dampers

Floor	No Control		w/ TMD		w/ ATMD		w/ MR			
							Passive Off		Clipped Optimal	
	$\lvert y_{s,i}\rvert$	$\lvert \ddot{y}_{s,i}\rvert$	$\lvert y_{s,i}\rvert$	$\lvert \ddot{y}_{s,i}\rvert$	$\lvert y_{s,i}\rvert$	$\lvert \ddot{y}_{s,i}\rvert$	$\lvert y_{s,i}\rvert$	$\lvert \ddot{y}_{s,i}\rvert$	$\lvert y_{s,i}\rvert$	$\lvert \ddot{y}_{s,i}\rvert$
	cm	cm/s^2	cm	cm/s^2	cm	cm/s^2	cm	cm/s^2	cm	cm/s^2
30	6.8	7.1	5.6	4.6	5.1	3.3	6.2	6.0	4.8	3.5
60	22.4	20.0	17.8	12.7	16.3	8.9	20.1	17.6	15.2	8.5
75	31.6	30.3	24.8	19.8	22.7	11.6	28.4	25.9	21.2	14.0
76	32.3	31.2	25.4	20.5	23.2	15.9	29.1	26.2	21.6	13.2

Table 3 RMS response quantities of 76-story building with various dampers

Floor	No Control		w/ TMD		w/ ATMD		w/ MR			
							Passive Off		Clipped Optimal	
	$\sigma_{y_{s,i}}$	$\sigma_{\ddot{y}_{s,i}}$	$\sigma_{y_{s,i}}$	$\sigma_{\ddot{y}_{s,i}}$	$\sigma_{y_{s,i}}$	$\sigma_{\ddot{y}_{s,i}}$	$\sigma_{y_{s,i}}$	$\sigma_{\ddot{y}_{s,i}}$	$\sigma_{y_{s,i}}$	$\sigma_{\ddot{y}_{s,i}}$
	cm	cm/s^2	cm	cm/s^2	cm	cm/s^2	cm	cm/s^2	cm	cm/s^2
30	2.25	2.02	1.48	1.23	1.26	0.90	1.89	1.71	1.17	0.77
60	7.02	6.42	4.79	3.72	4.08	2.81	6.15	5.42	3.77	2.28
75	9.92	9.14	6.75	5.38	5.74	3.34	8.67	7.72	5.29	3.52
76	10.10	9.35	6.90	5.48	5.86	4.70	8.87	7.89	5.41	3.41

Table 4 Control performance indices for various dampers

Criteria	w/ MR Dampers		w/ TMD (Yang et al. 2000)	w/ ATMD (Yang et al. 2000)
	Passive Off	Clipped Optimal		
J_1	0.84	0.38	0.58	0.36
J_2	0.84	0.36	0.58	0.41
J_3	0.87	0.53	0.68	0.57
J_4	0.87	0.53	0.68	0.58
J_7	0.85	0.46	0.65	0.38
J_8	0.88	0.44	0.63	0.43
J_9	0.90	0.66	0.78	0.71
J_{10}	0.90	0.67	0.79	0.72

Table 5 Maximum damper forces

Locations (Floor)	No. of Dampers	Forces (kN)	
		Passive Off	Clipped Optimal
63	2	41.5	400.0
66	7	145.3	1261.3
70	5	105.1	1000.0
73	4	83.1	800.0
76	3	62.5	600.0

Table 6 Performance of MR dampers for various wind force levels

Criteria	Force Levels			
	$0.5F_{WD}$	F_{WD}	$1.5F_{WD}$	$2.0F_{WD}$
RMS Responses				
J_1	0.34	0.38	0.44	0.49
J_2	0.34	0.36	0.43	0.49
J_3	0.50	0.53	0.57	0.60
J_4	0.50	0.53	0.57	0.61
Peak Responses				
J_7	0.41	0.46	0.53	0.58
J_8	0.44	0.44	0.53	0.59
J_9	0.64	0.66	0.69	0.71
J_{10}	0.65	0.67	0.70	0.72